特別掲載

Computer Processing of the Scintigraphic Image using Digital Filtering Techniques

By

Michimasa Matsuo

Department of Radiology, Kobe University, School of Medicine, Kobe, Japan
(Director: Prof. Kazuyuki Narabayashi)

Research Code No.: 208

Key Words: *Digital filtering, FIR digital filter, IIR digital filter, Image processing, Frequency response*

DIGITAL FILTERING による RI 画像 COMPUTER PROCESSING の研究

神戸大学医学部放射線医学教室
松　尾　導　昌

（昭和50年11月4日受付）
（昭和50年12月18日最終原稿受付）

ディジタルフィルタ理論を検討し，ＲＩ画像処理に応用した．すなわち，一次元ＦＩＲディジタルフィルタ（以下ＤＦと略す）の周波数特性を求め，これが線形な位相特性をもつ条件を算出した．これら条件を満足する一次元ＦＩＲ低域通過ＤＦを用い，シミュレーションをおこなつた結果，理論値に極く近以した実際値を得，算出された条件の有用性を確認した．

さらに線形一次元ＦＩＲ低域通過ＤＦの積の形で導出できる可分形の線形二次元ＦＩＲ低域通過ＤＦを考え，現在広く行われているスムージングを線形可分形二次元ＦＩＲ低域通過ＤＦの一実現形として捉えた．10種のカットオフ（3dB 低下）周波数を有するＦＩＲ低域通過ＤＦを設計し，その理論的振幅特性を求めた．

これらＦＩＲ低域通過ＤＦと，線形二次元 IIR 低域通過ＤＦ（一次のバタワース型）をシンチカメラ・ミニコンピュータ・オンライン・システムにアセンブラ言語を用いて実現し，cold targets を有するファントムＲＩ画像の処理をおこなつた．その結果，出力画像と用いられたＤＦの振幅特性，特に 3dB 低下周波数との間には密接な関連がみられ，換言すれば，ＤＦの理論的振幅特性からその出力画像が予期しうることが確認された．

さらに上記ファントム実験より，^{198}Au-コロイドを用いた肝臓シンチグラムに適当と考えられるＦＩＲ低域通過ＤＦを求め，臨床的応用をおこなつた．臨床的にも真の欠損像の検出と偽欠損像ならびに統計的変動による雑音の除去にこのＦＩＲ低域通過ＤＦが有用であることを確認した．

これら研究により，ディジタルフィルタリング

理論を的確に把握し，特にそのＤＦの周波数特性を充分把握しておこなうディジタルフィルタリング手法は，ＲＩ画像処理において重要かつ有意義なものであることを確認した．

Abstract

The theory of digital filtering was studied as a method for the computer processing of scintigraphic images. The characteristics and design techniques of FIR digital filters with linear phase were examined using the z-transform. The conventional data processing method, smoothing, could be recognized as one kind of linear phase FIR low-pass digital filtering. filtering. Ten representatives of FIR low-pass digital filters with various cut-off frequency were scrutinized from the frequency domain in one-dimension and two-dimension. These filters were applied to the phantom studies with cold targets, using a Scinticamera-Minicomputer on-line System.

These studies revealed that the resultant images had direct connection with the magnitude response of the filter, that is, they could be estimated fairly well from the frequency response of the used digital filter. The filter, which was estimated from phantom studies as optimal for liver scintigrams using ^{198}Au-colloid, was successfully applied in clinical use for detecting true cold lesions and at the same time for eliminating spurious images.

I. Introduction

With the rapid progress in the digital computer technology, primarily as a result of the development in digital integrated circuits, computer processing technique has been gradually adopted in the radiological field. Particularly in radioisotope scintigraphy, a number of studies have been performed on image processing. Work has been carried out on data smoothing to reduce random count fluctuations by the spatial averaging technique[8] in order to increase the signal-to-noise ratio (S/N ratio) which improves the picture quality when noisy images are viewed. Improvement of spatial resolution has been attempted by means of iterative approximation methods[7], differential operator methods[14)15], the Fourier transform method[28], matched filter method and optimal filter method[26].

The digital computer processes only discrete data. In the communication engineering filed, the digital filtering has been applied to extract necessary informations from discrete data.

The techniques for designing one-dimensional digital filters have been investigated for several years, and are now fairly well established[2)3)9)22)23]. Two of the most common classes of one-dimensional digital filters are usually called recursive and nonrecursive filters, respectively. An alternative terminology, "infinite impulse response" (IIR) and "finite impulse response" (FIR) has recently been proposed[20]. IIR filters can be realized by a number of methods and must take into account the stability and linearity of phase response[4)5)6)11)12)13)16)25]. On the other hand, in the case of FIR digital filters, the problem of stability does not exist in one-dimension as the z-transform is a finite polynomial. Design techniques in one-dimension can often be directly extended to two or more dimensions by appropriate modifications of the design procedure[1)17)18].

Two-dimensional digital filtering has been utilized for processing seismic records[27] and gravity magnetic data[29]. Two-dimensional digital filtering can also be used for enhancing photographic data such as weather photos, air photos and medical x-rays[24].

The main purposes of this paper is to apply the two dimensional digital filtering techniques to the

processing of the scintigraphic images, giving the theoretical basis to the present computer processing methods of the scintigraphic images (for example smoothing), by scrutinizing the digital informations not only from the space domain, but also from the frequency domain through z-transform.

II. Theory of Digital Filtering

[1] Digital Filtering

[A] IIR Filters

A one-dimensional digital filter is characterized by the following difference equation:

$$y(i)=\sum_{n=0}^{N-1}h_n x(i-n)+\sum_{n'=1}^{N'-1}h'_{n'}y(i-n') \tag{2.1}$$

where $\{x(i)\}$ is the input sequence and $\{y(i)\}$ is the output sequence. If $h'_{n'} \neq 0$ the system is called an infinite impulse response digital filter, or in short, an IIR filter. The z-transform*1 of (2.1) is given by

$$\begin{aligned}\sum_{i=0}^{\infty}y(i)z^{-i}&=\sum_{i=0}^{\infty}\Big(\sum_{n=0}^{N-1}h_n x(i-n)\Big)Z^{-i}\\&\quad+\sum_{i=0}^{\infty}\Big(\sum_{n'=1}^{N'-1}h'_{n'}y(i-n')\Big)Z^{-i}\\&=\sum_{n=0}^{N-1}h_n\sum_{i=0}^{\infty}x(i-n)Z^{-i}\\&\quad+\sum_{n'=1}^{N'-1}h'_{n'}\sum_{i=0}^{\infty}y(i-n')Z^{-i}\quad .\end{aligned} \tag{2.2}$$

When $x(i-n)=0$, for $i<n$, the z-transform of $x(i-n)$ is equivalent with the product of the z^{-n} and the z-transform of $x(i)$. Accordingly, (2.2) yields

$$Y(Z)=\sum_{n=0}^{N-1}h_n Z^{-n}X(Z)+\sum_{n'=1}^{N'-1}h'_{n'}Z^{-n'}Y(Z)\ . \tag{2.3}$$

Then

$$Y(Z)=H(Z)X(Z) \tag{2.4}$$

where

$$H(Z)=\frac{\sum_{n=0}^{N-1}h_n Z^{-n}}{1-\sum_{n'=1}^{N'-1}h'_{n'}Z^{-n}}\ . \tag{2.5}$$

H(z) is called the transfer function of the digital filter, and determines the characteristics of the system. Accordingly, the z-transform of the output y(i) of this system is the product of the z-transform of the input x(i) and H(z). In other words, H(z) is given by the ratio of the z-transform of the output to that of the input.

---

*1 A. One-dimensional z-transform

The z-transform of $\{x_n\}$ is defined as; $X(Z)=\sum_{n=0}^{\infty}x_n z^{-n}$.

The z-transform of a sequence may be viewed as a unique representation of that sequence in the complex z plane. If the z-transform is evaluated on a circle of unit radius, i.e., $z=e^{j\omega}$, then

$$X(z)|_{z=e^{j\omega}}=X(e^{j\omega})=\sum_{n=-\infty}^{\infty}x_n e^{-j\omega n}\ .$$

which is the Fourier transform of the sequence ($x_n=0$, $n<0$).

B. Two-dimensional z-transform

The z-transform of $\{x_{n1,n2}\}$ is defined as;

$$X(z_1,z_2)=\sum_{n_1=0}^{\infty}\sum_{n_2=0}^{\infty}x_{n1,n2}z_1^{-n_1}z_2^{-n_2}\ .$$

[B] FIR Filters

If the sequence $\{h'_{n'}\}$ is zero, i.e., an output y(i) is defined only by the inputs, x(i), x(i-1), ..., x(i-n), (2.1) becomes

$$y(i)=\sum_{n=0}^{N-1}h_n x(i-n)\,. \tag{2.6}$$

Then, the transfer function H(z) arrives at

$$H(Z)=\sum_{n=0}^{N-1}h_n Z^{-n}\,. \tag{2.7}$$

In this case, the system is called a finite impulse response digital filter*2, or in short an FIR filter.

When the input is a sampled discrete sequence of the complex sinusoidal wave

$$X(i)=e^{ij\omega} \tag{2.8}$$

the output y(i) is derived by substituting x(i) of (2.8) into (2.6) as

$$\begin{aligned} y(i)&=\sum_{n=0}^{N-1}h_n e^{j\omega(i-n)}\\ &=\sum_{n=0}^{N-1}h_n e^{ji\omega}e^{-jn\omega}\\ &=e^{ji\omega}H(e^{j\omega})\\ &=X(i)H(e^{j\omega})\,. \end{aligned} \tag{2.9}$$

Consequently, when the sinusoidal wave of (2.8) is applied at the input of this system, the output sequence is the product of x(i) and $H(e^{j\omega})$. In other words, y(i) is $|H(e^{j\omega})|$ times of x(i) in the magnitude and is at $\mathrm{Arg}(H(e^{j\omega}))$ shifted in the phase. $|H(e^{j\omega})|$ is called the magnitude response of the digital filter, and $\mathrm{Arg}(H(e^{j\omega}))$ is the phase response. Since $e^{j\omega}=e^{j(\omega+2\pi)}$, $H(e^{j\omega})$ is noticed as a periodic function with the period of 2π. This is practically significant in the region $0<\omega<\pi$ from the sampling theorem. In (2.7), when the input is the unit impulse, the output is the $\{h_n\}$ itself. In other words, $\{h_n\}$ is called the impulse response, decides the characteristics of the digital filter.

A similar theory is also obtained for the two-dimensional case, in which the input and output arrays are expressed as $x(i_1, i_2)$ and $y(i_1, i_2)$, respectively, and the transfer function is $H(z_1, z_2)$.

[2] Theory of FIR Filters with Linear Phase

[A] Phase Linearity

In the processing of images, linearity of the phase response of the digital filter is necessary. In this section, the phase linearity is discussed.

Let $\{h_n\}$ be a causal finite duration sequence defined over the interval $0\leqq n\leqq N-1$. The Fourier transform of $\{h_n\}$ is written as

$$H(e^{j\omega})=\sum_{n=0}^{N-1}h_n e^{-j\omega n}\,. \tag{2.10}$$

This equation is identical with the frequency response of the FIR filter. $H(e^{j\omega})$ is expressed in terms of its magnitude and phase, i.e.,

$$H(e^{j\omega})=\pm|H(e^{j\omega})|e^{j\theta(\omega)}\,. \tag{2.11}$$

It is seen from (2.10) that the magnitude of the Fourier transform is a symmetric function, and the phase is an antisymmetric function, i.e.,

*2Recursive digital filters will be dealt with in a separate research report.

$$|H(e^{j\omega})|=|H(e^{-j\omega})| \quad 0\leqq\omega\leqq\pi$$

$$\theta(\omega)=-\theta(-\omega) \ . \tag{2.12}$$

When the constraint of linear phase is imposed, $\theta(\omega)$ is of the form

$$\theta(\omega)=-N'\omega \quad -\pi\leqq\omega\leqq\pi \tag{2.13}$$

where N′ is a constant phase delay in the samples. In this case, (2.11) can be written in the form

$$H(e^{j\omega})=\sum_{n=0}^{N-1}h_n e^{-j\omega n}=\pm|H(e^{j\omega})|e^{-jN'\omega} \ . \tag{2.14}$$

From (2.14), two equations are obtained as follows:

$$\pm|H(e^{j\omega})|\cos(N'\omega)=\sum_{n=0}^{N-1}h_n\cos\omega n \tag{2.15}$$

$$\pm|H(e^{j\omega})|\sin(N'\omega)=\sum_{n=0}^{N-1}h_n\sin\omega n \ . \tag{2.16}$$

Eliminating $\pm|H(e^{j\omega})|$ from (2.15) and (2.16), we arrive at

$$\frac{\sin(N'\omega)}{\cos(N'\omega)}=\tan(N'\omega)=\frac{\sum_{n=0}^{N-1}h_n\sin\omega n}{\sum_{n=0}^{N-1}h_n\cos\omega n} \tag{2.17}$$

$$=\frac{\sum_{n=1}^{N-1}h_n\sin\omega n}{h_0+\sum_{n=1}^{N-1}h_n\cos\omega n} \ . \tag{2.18}$$

Let $N'=0$. It follows then

$$0=\frac{\sum_{n=1}^{N-1}h_n\sin\omega n}{h_0+\sum_{n=1}^{N-1}h_n\cos\omega n} \ . \tag{2.19}$$

The only solution of (2.19) is that h_0 be arbitrary and $h_n=0$ for $n\neq 0$, which is not very useful. When $N'\neq 0$, (2.18) can be rewritten as

$$\sum_{n=0}^{N-1}h_n\sin(N'-n)\omega=0 \ . \tag{2.20}$$

One solution of (2.20) is the following set of conditions:*3

$$\begin{aligned} &N'=(N-1)/2 \\ &h_n=h_{N-1-n} \end{aligned} \qquad 0\leqq n\leqq N-1 \ . \tag{2.21}$$

In this case, the filter has both constant group delay and constant phase delay.

[B] Frequency Response of Linear Phase FIR Filters

(1) N odd

When N is odd, (2.10) can be written as

$$H(Z)=\sum_{n=0}^{N-1}h_n Z^{-n}=Z^{-\frac{N-1}{2}}\{h_{\frac{N-1}{2}}+\sum_{n=1}^{\frac{N-1}{2}}h_{\frac{N-1}{2}-n}(Z^{-n}+Z^{n})\} \tag{2.22}$$

$$H(e^{j\omega})=e^{-j\omega\frac{N-1}{2}}\{h_{\frac{N-1}{2}}+2\sum_{n=1}^{\frac{N-1}{2}}h_{\frac{N-1}{2}-n}\cos\omega n\} \tag{2.23}$$

*3 In this study, FIR filters with a symmetrical impulse response are discussed. However, linear phase FIR filters with an asymmetrical impulse response are practically useful, but are not referred here.

where

$$N' = (N-1)/2.$$

Consequently, the magnitude response is

$$|H(e^{j\omega})| = |h_{N'} + 2\sum_{n=1}^{N'} h_{N'-n} \cos \omega n| \ . \tag{2.24}$$

If the constraint that the magnitude response be zero at $\omega = \pi$ is imposed, (2.24) becomes

$$|h_{N'} + 2\sum_{n=1}^{N'} h_{N'-n} (-1)^n| = 0 \ . \tag{2.25}$$

When $N = 3$, and $h_0 = h_2 = 1$, then

$$h_1 = 2. \tag{2.26}$$

When $N = 5$, and $h_0 = h_4 = 1$, then

$$|h_2 + 2 - 2h_1| = 0. \tag{2.27}$$

One solution of (2.27) is

$$h_1 = h_3 = 5, \quad h_2 = 8. \tag{2.28}$$

The phase response is (Fig. 1)

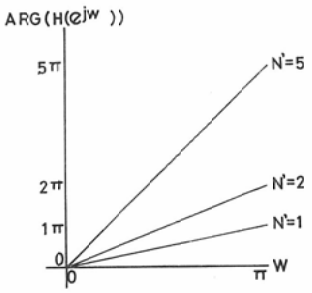

Fig. 1　Phase responses of a one-dimensional linear phase FIR digital filter.

$$\mathrm{Arg}(H(e^{j\omega})) = -N'\omega. \tag{2.29}$$

The group delay of (2.23) is N'.

(2)　N even

When N is even, (2.10) can be written as

$$H(Z) = \sum_{n=0}^{N-1} h_n Z^{-n} = Z^{-N'} \{\sum_{n=1}^{N'} h_{N'-n} (Z^{-n} + Z^n)\}$$

$$H(e^{j\omega}) = e^{-j\omega\frac{N-1}{2}} \{2\sum_{n=1}^{\frac{N}{2}} h_{\frac{N}{2}-n} \cos[\omega_{(n-1/2)}]\} \tag{2.30}$$

where

$$N'' = \frac{N}{2}.$$

The magnitude response is

$$|H(e^{j\omega})| = 2|\sum_{n=1}^{N'} h_{N'-n} \cos[\omega(n-1/2)]| \ . \tag{2.31}$$

The phase response is

$$\mathrm{Arg}(H(e^{j\omega}))=-\frac{N-1}{2}\omega=-N'\omega$$
$$=-(N''-1/2)\omega\ . \tag{2.32}$$

which shows that the group delay is $(N''-1/2)$.

[3] Two-Dimensional FIR Digital Filters

Two-dimensional FIR digital filter with linear phase, $H(z_1, z_2)$ can be simply designed as the product of the transfer functions of two one-dimensional FIR digital filters with linear phase, $H_1(z_1)$ and $H_2(z_2)$*4. In this case, the magnitude response is

$$|H(e^{j\omega_1}, e^{j\omega_2})|=|H_1(e^{j\omega_1})||H_2(e^{j\omega_2})|\ . \tag{2.33}$$

and the phase response is (Fig. 2)

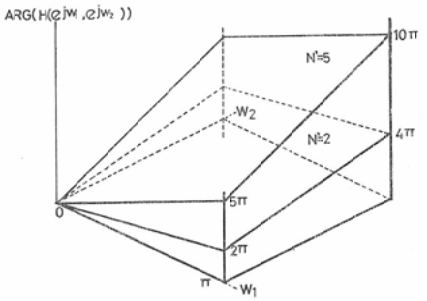

Fig. 2 Phase responses of a two-dimensional linear phase FIR digital filter.

$$\mathrm{Arg}(H(e^{j\omega_1}, e^{j\omega_2}))=\mathrm{Arg}(H_1(e^{j\omega_1}))+\mathrm{Arg}(H_2(e^{j\omega_2}))\ . \tag{2.34}$$

This is one of the realizing methods of two-dimensional FIR digital filters with linear phase, and is simple to use. It is also easy to determine the frequency response of the separable two-dimensional filter.

Two-dimensional digital filtering of this class is performed by the following procedures:

First processing with the one-dimensional filter, $H_1(z_1)$, an intermediate output sequence is obtained. Next, this output sequence is processed with the one-dimensional filter $H_2(z_2)$, to yield the desired output.

This approach has been found to be quite practical in the computer processings of the scintigrams as it has reduced the programming steps and processing time. In this paper $H_2(z_2)$ was set as the same as $H_1(z_1)$.

III. Instruments

[1] Design of Linear Phase FIR Low-Pass Filters

Based on the theory, ten linear phase FIR low pass filters are designed which can be easily and practically applied to smoothing. These are designed under the constraints as follows:

(1) N is odd, and less than or equal to seven.

(2) $\{h_n\}$ is composed of integers.

The impulse responses of the designed filters in one-dimension are as follows:

*4 The same procedures can be applied to the IIR digital filters.

Filter I　　$\{h_n\} = 1, 1, 1, 1, 1, 1, 1$
Filter II　　$\{h_n\} = 1, 1, 1, 1, 1$
Filter III　　$\{h_n\} = 1, 1, 2, 1, 1$
Filter IV　　$\{h_n\} = 1, 1, 3, 1, 1$
Filter V　　$\{h_n\} = 1, 1, 4, 1, 1$
Filter VI　　$\{h_n\} = 1, 5, 8, 5, 1$
Filter VII　　$\{h_n\} = 1, 1, 1$
Filter VIII　　$\{h_n\} = 1, 2, 1$
Filter IX　　$\{h_n\} = 1, 3, 1$
Filter X　　$\{h_n\} = 1, 4, 1$

The magnitude responses of these digital filters in one-dimension are calculated based on (2.24) and are demonstrated in Fig. 3.

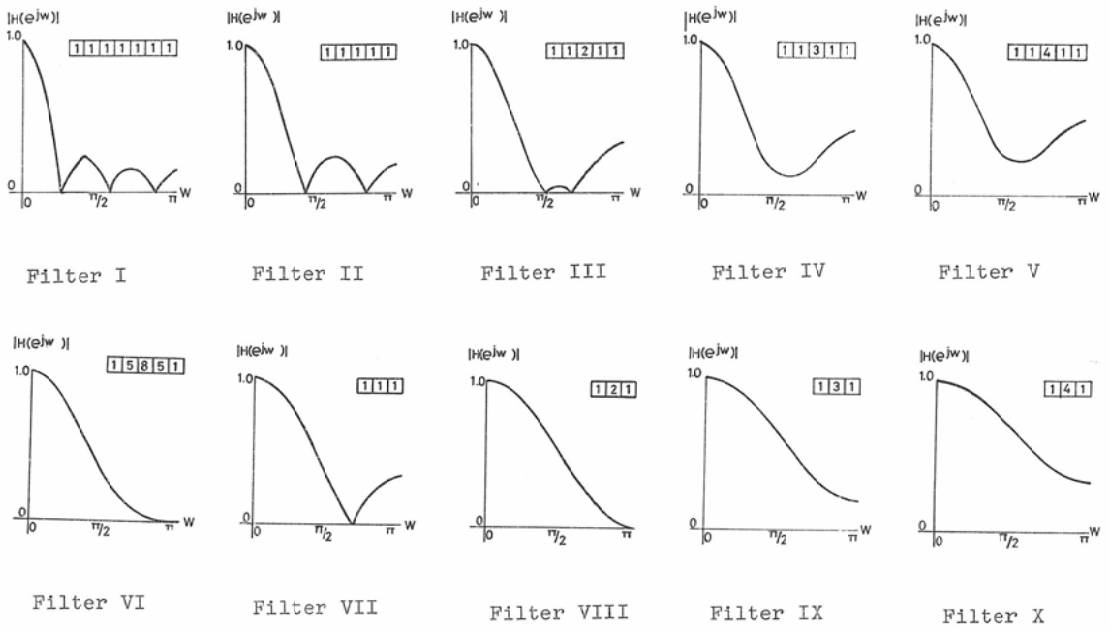

Fig. 3　Magnitude responses of one-dimensional FIR digital filters (Filters I–X).

Setting the cut-off frequency in this paper as the frequency at which the magnitude is just 3dB less than that at zero frequency, the cut-off frequency of the ten filters is calculated using (2.24) and given in Table 1. In order to understand the frequency response of above mentioned filters in two-dimension, Fig. 4 shows the magnitude response of Filters II, VI, VII and VIII in two dimension. Other's pictures are excluded in this paper.

[2] A Scinticamera-Minicomputer on-line System and Programming of Digital Filtering

Figure. 5 shows the on-line system used in nuclear medicine in Kobe University. The data are transferred from the scinticamera (Toshiba Gamma Camera, Model GCA-101) to the minicomputer (Tosbac

Table 1. Cut-off Frequency of Filters I–X

Filter	Cut-off Frequency	ω
I	0.0663	0.1325π
II	0.0902	0.1803π
III	0.0998	0.1996π
IV	0.1090	0.2179π
V	0.1178	0.2356π
VI	0.1381	0.2761π
VII	0.1553	0.3105π
VIII	0.1821	0.3641π
IX	0.2069	0.4137π
X	0.2307	0.4613π

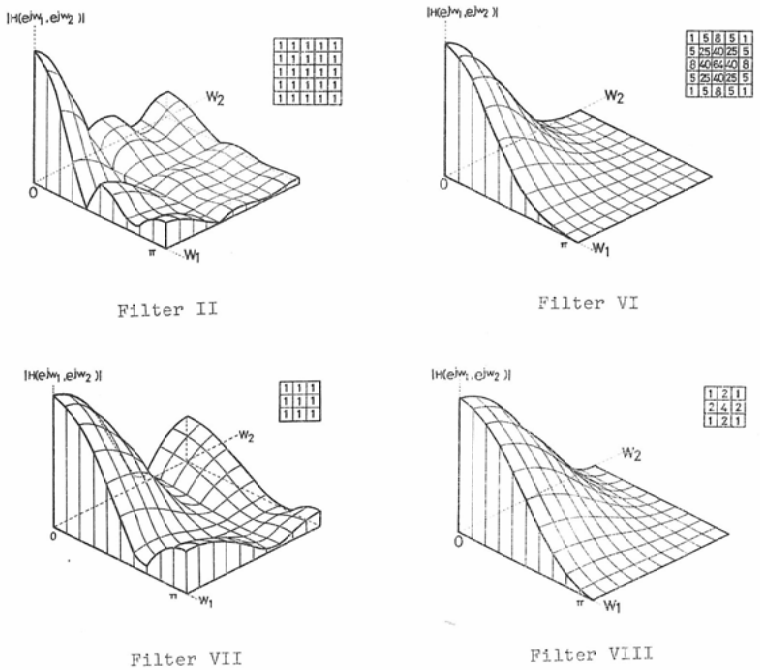

Filter II　　Filter VI

Filter VII　　Filter VIII

Fig. 4 Magnitude responses of two-dimensional FIR digital filters.

40 with 24 K bytes memory) through the A/D converter and the computer interface. The DAP-5000 data processing system is provided as software for the usual data processing. The resultant image is displayed upon the CRT under the control of the minicomputer.

A program for the digital filtering was written by the author with Assembler language. It was then assembled to make the object program, which was loaded into the minicomputer. By this procedure, on-line digital filtering became possible with arbitrary $\{h_{n1}, h_{n2}\}$.

IV. Simulation Study

In order to confirm that the practical results of low-pass FIR digital filtering is essentially the same as the theoretical values, the following simulation was performed.

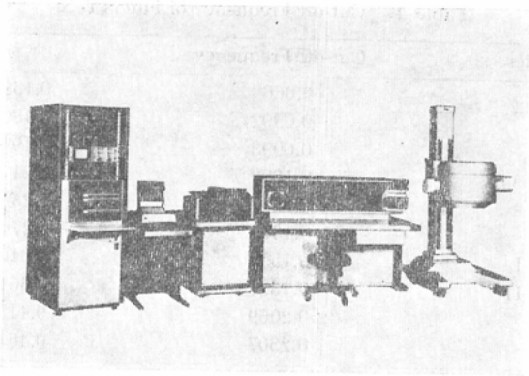

Fig. 5　Scinticamera-minicomputer on-line system.

[A]　Method

(1)　Set the impulse response of the examined filters as follows:

$\{h_n\} = 1, 5, 8, 5, 1$ $(n = 0, 1, \ldots, 4)$.

(2)　Calculate the theoretical frequency response of the filter.

(3)　Make the wave, which is the sum of various cosine waves:

$$\sum_{n=0}^{10} \cos\frac{n\pi}{10}. \qquad (3\text{-}1)$$

(4)　The input data sequence is set as the discrete value sampled at the point when $n = 0, 1, \ldots, 10$ in (3-1).

(5)　The digital filter is applied, and the DFT (discrete Fourier transform) of the output sequence is performed to give the magnitude and the phase at the point of $\omega = n\pi/10$ $(n = 0, 1, \ldots, 10)$.

(6)　Compare the result of the DFT of the output sequence with the theoretical value.

These procedures were performed with FACOM 230-35 in Computer Center of Kobe University.

[B]　Results

A comparison of the experimental and theoretical values is shown in Table 2.　As seen, the practical

Table 2.　Result of the simulation study

Magnitude response			Phase response		
ω	Theoretical value	DFT of the output	ω	Theoretical value	DFT of the output
0	1.0000000	0.9999924	0	0.0 (0.0)	0.0
$\pi/10$	0.9564292	0.9564262	$\pi/10$	−0.2 (−0.2)	−0.1999993
$2\pi/10$	0.8354950	0.8354027	$2\pi/10$	−0.4 (−0.4)	−0.4000008
$3\pi/10$	0.6629912	0.6629849	$3\pi/10$	0.4 (−0.6)	0.3999984
$4\pi/10$	0.4736069	0.4736076	$4\pi/10$	0.2 (−0.8)	0.1999976
$5\pi/10$	0.3000007	0.2999978	$5\pi/10$	0.0 (−1.0)	0.0000010
$6\pi/10$	0.1645902	0.1645886	$6\pi/10$	−0.2 (−1.2)	−0.1999997
$7\pi/10$	0.0752060	0.0752043	$7\pi/10$	−0.4 (−1.4)	−0.4000033
$8\pi/10$	0.0263933	0.0263929	$8\pi/10$	0.4 (−1.6)	0.3999966
$9\pi/10$	0.0053736	0.0053728	$9\pi/10$	0.2 (−1.8)	0.1999791
π	0.0000000	0.0000021	π	0.0 (−2.0)	0.0000066

values coincided well with the theoretical values. Consequently, it is confirmed that low-pass FIR digital filtering based on the theory outlined in section II is of practical use.

V. Phantom Studies on Cold Targets

First, phantom studies on cold targets were performed by the ten low-pass FIR digital filters [Study V-1]. Then in order to understand and to ascertain the relation of the magnitude response of the filters with resultant images, digital filtering by linear phase IIR (Butterworth type) low-pass digital filters were used [Study V-2]. The detail about the design technique of linear phase IIR digital filters is not given in this paper but will be referred in [10].

Last, the S/N ratio of each filtered image by Filters I–X.

[Study V-1]

[A] Method

A slice phantom with cold targets of various diameters (Fig. 6) was filled with 300 μCi of ^{198}Au-

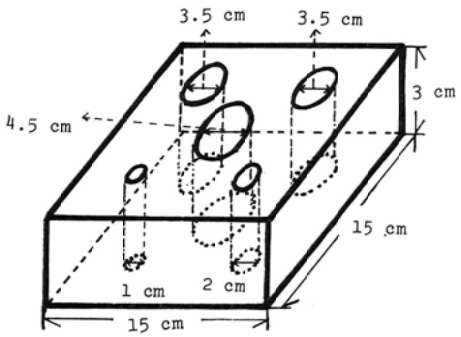

Fig. 6 Schematic representation of a slice phantom.

colloid solution. The cold targets of 4.5 cm in diameter was named in this paper as Cold Target I and those of 3.5 cm, 2 cm, and 1 cm were named as Cold Targets II, III, and IV, respectively. A collimator with 1000 holes was attached to the gamma camera. The original scintigram was taken on a polaroid film. It was simultaneously converted to discrete data and stored in the minicomputer memory as 64 × 64 matrix two-dimensional discrete data. The stored counts were about 240K counts. (In this state, one of the values of the 64 × 64 matrix almost reached 255 counts.) Low-pass FIR digital filtering was performed by Filters I–X. The resultant images were displayed on the CRT as digitalized (64 × 64 matrix) images and recorded on polaroid films.

[B] Results (Fig. 7)

(1) Processing by Filter I revealed Cold Targets I and II clearly. But, neither Cold Targets III nor IV could be distinctly seen.

(2) By Filter II, Cold Targets I and II were clearly visualized. Cold Target III was dimly shown, but it was slightly difficult to notice Cold Target IV.

(3) By Filters III, IV and V, Cold Targets I and II were distinct. But Cold Tagets III and IV were dimly demonstrated. Cold Targets III and IV were more clearly visualized by Filter IV than by Filters III and less distinct than by Filter V.

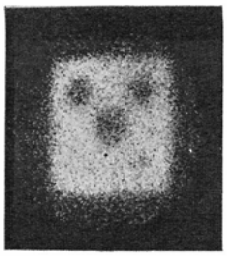

original scintigram

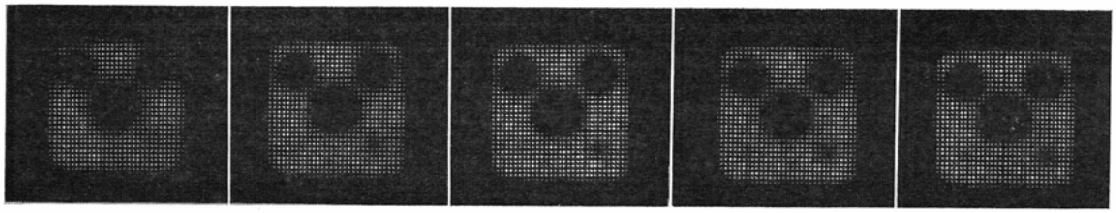

by Filter I　by Filter II　by Filter III　by Filter IV　by Filter V

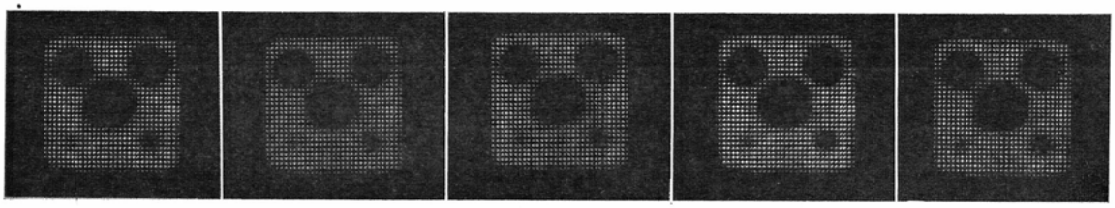

by Filter VI　by Filter VII　by Filter VIII　by Filter IX　by Filter X

Fig. 7　Filtered scintigrams by Filters I–X.

(4)　By Filter VI, Cold Targets I–IV were all sharply visualized without spurious cold images.

(5)　By Filters VII–X, Cold Targets I–IV were all clear. But, the spurious cold images appeared dimly in the result by Filter VII and increased gradually with the increase of Filter number. This fact suggested that noise from statistical fluctuations in radionuclide distribution or others, passed through these filters.

(6)　In this phantom study, Filter VI was considered optimal to obtain true images of the cold targets without spurious cold nor mottled images.

(7)　By this phantom study, it was inferred that the magnitude response of the filter in the frequency domain could have much effect on the resultant image in the space domain.

[Study V-2]

From [Study V-1], the relation of the resultant image and the magnitude response of digital filters was suggested. To ascertain this, the following phantom study was performed using linear phase IIR low-pass digital filters of first order Butterworth type.

[A]　Method

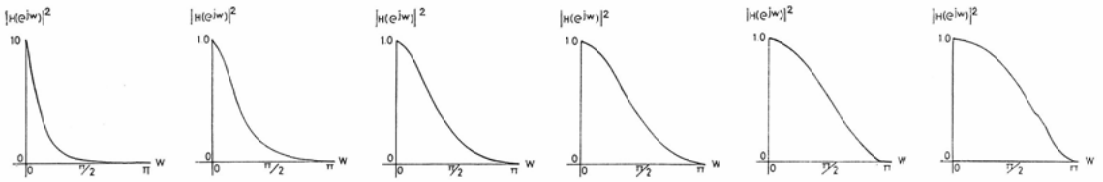

Fig. 8 Magnitude responses of one-dimensional IIR digital filters (Filters A–F).

Table 3. Cut-off Frequency of Filters A–F

Filter	Cut-off Frequency	ω
A	0.05	0.1π
B	0.10	0.2π
C	0.15	0.3π
D	0.20	0.4π
E	0.25	0.5π
F	0.30	0.6π

Employed IIR filters were named as Filters A–F, whose magnitude in one-dimension is shown, respectively in Fig. 8. Cut-off frequency of Filters A–F is given in Table 3. The same procedures were performed as in [Study V-1] using Filters A–F. In order to distinguish the resultant images by IIR filters from those by FIR filters, images were turned over, then the site of Cold Target III changed place with Cold Target IV comparing to the case of [Study V-1].

[B] Results

The original image was shown in Fig. 9. The filtered images by Filters A–F were displayed respec-

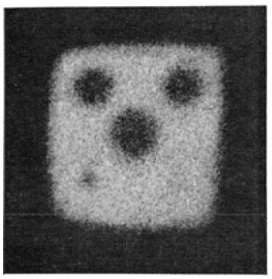

Fig. 9 Original scintigram.

tively in Fig. 10.

(1) By Filter A, neither Cold Target III nor IV could be visualized.

(2) By Filter B, Cold Target IV could not be demonstrated.

(3) By Filter C, Cold Target III appeared clearly and Cold Target IV was dimly noticed. And moreover, no spurious cold images were seen.

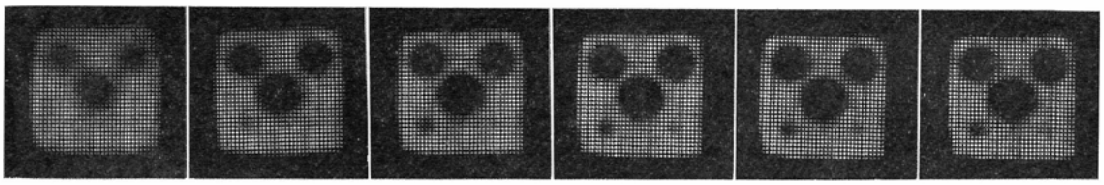

by Filter A　by Filter B　by Filter C　by Filter D　by Filter E　by Filter F

Fig. 10　Filtered scintigrams by Filters A–F.

Table 4.　Cut-off Frequency of Filters a–d

Filter	Cut-off Frequency	ω
a	0.1250	0.2500π
b	0.1500	0.3000π
c	0.1750	0.3500π
d	0.1900	0.3800π

(4)　By Filter D, Cold Target IV was visualized more clearly.　But the mottled images of statistical fluctuations dimly appeared.

(5)　By Filters E and F, Cold Targets I–IV were all clearly visualized but the spurious images also appeared.

(6)　From the result above, it was suggested that the optimal cut-off frequency was near 0.15.

(7)　From the results of [Study V-1] and [Study V-2], it was ascertained that the resultant image had direct relation with the magnitude response of filters, especially their cut-off frequency.

[Study V-2′]

In two studies of [Study V-1] and [Study V-2], 240K counts were stored, which made the original stored data in the minicomputer composed of less noise.　So even in the resultant images by filters with high cut-off frequency, the spurious images were not so conspicuous.　But in a practical case, a different condition such as in smaller counts may occur.　To examine this problem in more detail, the following study was performed.

[A]　Method

The similar study was performed as in [Study V-2] except that 120K counts were stored in the minicomputer and that linear phase IIR low-pass digital filters of first order Butterworth type (Filters a–d) was used, whose cut-off frequency was 0.125 ($\omega = 0.25\pi$), 0.15 ($\omega = 0.3\pi$), 0.175 ($\omega = 0.35\pi$), 0.19 ($\omega = 0.38\pi$), respectively.

[B]　Results

Results were given in Fig. 11.

(1)　Neither Filter-a nor Filter-b visualized Cold Target IV.　But, it was considered that those two filters were almost sufficient to eliminate the spurious images.

(2)　By Filters-c and d, Cold Target IV was dimly visualized.　But spurious cold images became appeared and slightly confusing the true images.

(3)　The results showed that the more the stored counts were, the less the spurious images were. And the less stored counts demanded the lower cut-off frequency of low-pass filters for eliminating spurious

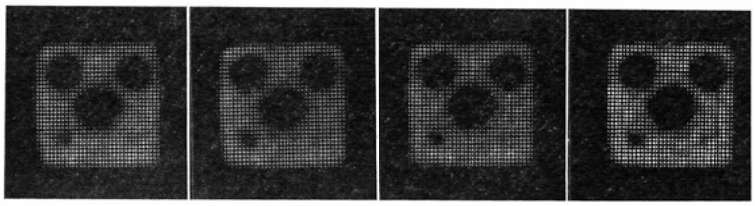

by Filter a by Filter b by Filter c by Filter d

Fig. 11 Filtered scintigrams by Filters a–d.

images, which led to more loss of true cold images.

[Study V-3]

This study was performed to know the change of S/N ratio of a RI image, after it was processed by Filters I–X.

[A] Method

The modulation transfer function (MTF) of the detector-collimator of the system was obtained using a line source which was filled with ^{198}Au-colloid and was set at 10 cm from the 1000 holes collimator. In order to make the calculation easier, this obtained MTF was supposed as the MTF in one-dimension of the system.

The S/N ratio of the original image was calculated in one-dimension and in two-dimension. And then the S/N ratio of each filtered image by Filters I–X was computed in one-dimension and in two-dimension, which was divided by the S/N ratio of the original image. By this normalizing procedures, each filtered image could be compared and evaluated, based on the theory of S/N ratio.

Table 5. Ratio of R_f/R_o

	R_f/R_o in two-dimension
original	1.000
Filter I	1.822
Filter II	2.159
Filter III	2.296
Filter IV	2.149
Filter V	1.975
Filter VI	2.533
Filter VII	2.455
Filter VIII	2.299
Filter IX	2.020
Filter X	1.814

R_f: the S/N ratio of filtered image
R_o: the S/N ratio of original image

[B] Results

As seen in the results (Table 5), the best S/N ratio of the filtered image was obtained by Filter VI among those by Filters I–X.

VI. Clinical Studies on Cold Targets

[A] Method

Based on the results of the phantom studies, Filter VI was used for the clinical application. And 300 μCi of ^{198}Au-colloid were used in all cases.

[B] Results

This has been applied to 30 cases without or with cold lesions in the liver, such as gallstones, metastatic tumors, hepatomas, etc.

[Case 1] Liver without Cold Lesions

The scintigram of a liver without space occupying lesions (56 y.o. male patient) was obtained. Fig. 12 shows the original scintigram and the filtered scintigram, in which no spurious cold lesions appeared all over the liver image.

[Case 2] Case of Gallstones in the Choledochus

A 60 y.o. male patient whose chief complaints was liver swelling and jaundice, was examined. He had been occasionally attacked by high fever over a period of 3 years. The filtered liver scintigram (Fig. 13) revealed clear cold lesions. The ERCP (Fig. 14) demonstrated the presence of gallstones in the choledochus. Accordingly, the cold spots were considered to have appeared as a result of dilation of biliary ducts. After the removal of four gallstones, the filtered scintigram of the liver (Fig. 15) revealed that the large cold lesions disappeared, suggesting that these cold images occurred as a result of marked dilatation of the biliary duct.

[Case 3] Case of Metastatic Tumors

A 64 y.o. male patient was diagnosed as suffering from sigmoid cancer. The liver was examined.

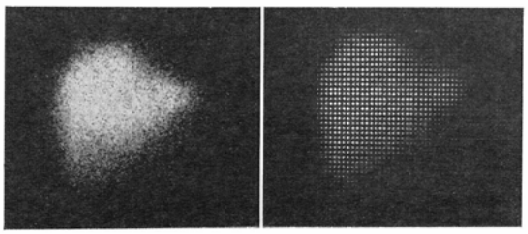

original　　filtered scintigram

Fig. 12. Clinical application to the case of a liver without space occupying lesions.

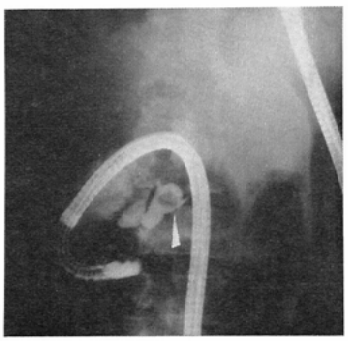

Fig. 14 ERCP findings before operation.

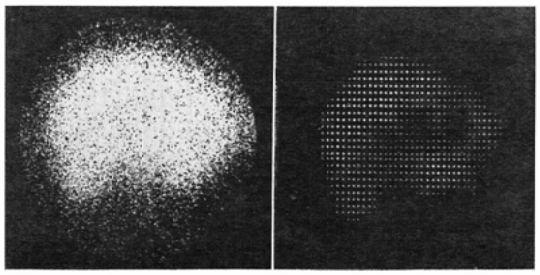

original　　filtered scintigram

Fig. 13 Clinical application to the case of gallstones in the choledochus.

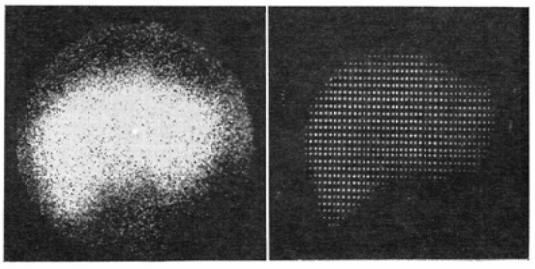

original　　filtered scintigram

Fig. 15 Scintigram of the patient of Fig. 13 after operation.

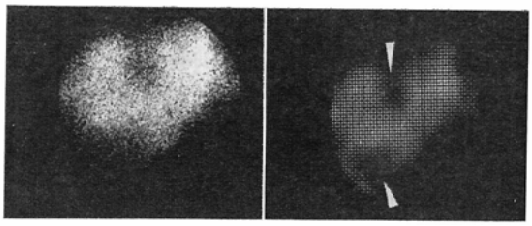

original filtered scintigram

Fig. 16 Clinical application to the case of multiple liver metastases from sigmoid cancer.

The original scintigram was given in Fig. 16. Filtered scintigram revealed cold metastatic lesions more clearly and existence of these metastases was confirmed by operation.

VII. Discussion

Digital image data (such as scintigraphic image) can be treated based on the digital filtering theory.

FIR digital filters with linear phase were adopted in this study. The principal advantages of FIR filters are as follows:

(1) It is easy to design FIR filters with exactly linear phase. This simplifies the approximation problem, since one can be concerned about only with approximating the arbitrary magnitude response.

(2) FIR filters realized nonrecursively, i.e., by direct convolution, are always stable.

(3) Round off noise can easily be reduced for nonrecursive realizations of FIR filters.

However, the following disadvantage must be considered: a long sequence in the impulse respon equired for adequately approximating sharp cut off filters with arbitrary magnitude response. This becomes a problem specifically when a short sequence or array of input data is to be handled, such as in the case of scintigraphic data.

In the present study, the symmetrical impulse response was used to satisfy the linearity. However, there exist linear phase FIR digital filters with asymmetrical impulse response. The conditions for these are:

$$N' = (N\text{-}1)/2$$

$$h_n = -h_{N-1-n}.$$

In this case, $|H(e^{j\omega})|$ is always zero at $\omega = 0$.

Frequency sampling methods, design techniques for linear phase FIR filters, such as the Window Method and the Optimal (in the sense of the Chebyshev approximation) Filter Design Methods, are available. They are not referred to in this study.

In this paper, Filter VI was selected for the clinical study from the following reasons.

(1) In order to be easily and practically applied to smoothing, the linear phase FIR low-pass filter is designed under the constraints as follows:

(a) N is odd, and less than or equal to seven.

(b) $\{h_n\}$ is composed of integers.

(2) From [Study V-1], the filtered image by Filter VI revealed all true cold targets with less spurious images.

(3) The cut-off frequency of Filter VI is 0.1381 ($\omega = 0.2761\pi$), which was ascertained to be best in [Study V-2] for revealing true cold targets with less spurious images.

(4) The magnitude response is much less in the higher frequency than in its cut-off, and it is zero at $\omega = \pi$.

(5) The S/N ratio was highest in [Study V-3].

And it was proved that Filter VI was very useful in clinical application.

But, as phantom studies reassured, the frequency characteristics or distribution of the signal and noise of the scintigraphic image are different, depending upon the stored counts. As seen in [Study V-2′], the lower cut-off frequency is necessary in case of less stored counts, in order to eliminate spurious images. Considering this fact, it is not so easy to decide the best filter when stored counts are not so adequately full, because the elimination of the spurious cold images is accompanied with loss of necessary informations of the true cold lesions. In this case of less counts, the filter with highest S/N ratio may not always be best in clinical application.

The problem about the case of less stored counts may well be solved by using much of radioisotope with short half life time and by making the one memory of the digital computer composed of many bits.

But, a line spread function, using the same system, is different depending upon the distance between a line source and a collimator. From this fact, it is considered difficult to decide the line spread function of the system when the three-dimensional structure with large volume is examined using the high energy radioisotope. This problem makes the calculation of S/N ratio more complicated and has not already been solved adequately.

In order to obtain the best filter for the clinical application to the large organ, such as the liver, the versatile and synthetic study, as seen in this article, might be necessary not only based on the S/N ratio but also on frequency characteristics (or cut-off frequency) of the designed filters.

VIII. Conclusion

Based on the theory of the digital filtering, the conventional smoothing could be recognized as one kind of linear phase FIR low-pass digital filtering. The optimal smoothing was examined by studying the connection of the resultant images and the frequency characteristics of the used smoothing. The resultant image, processed by the selected filter as optimal, showed high S/N ratio. And this filter was successfully applied in clinical use for detecting true cold lesions with elimination of spurious images.

IX. Acknowledgment

The author is indebted to many staff members of Kobe University, School of Medicine, Department of Radiology, and the Faculty of Engineering. In particular, he wishes to express his thanks to Professor Kazuyuki Narabayashi, associate Professor Kotaro Hirano and associate Professor Shoji Nishiyama for their helpful and constructive advice. And he is thankful to Dr. Takeshi Iinuma of National Institute of Radiological Sciences, for his valuable suggestion.

References

1) Cochran, W.T., Cooley, J.W., Favin, D.L., Helms, H.D., Raenel, R.A., Lang, W.W., Maling, G.C., Nelson, Jr. D.E., Rader, C.M. and Welch, P.D.: "What is the fast Fourier transform?," Proc. IEEE, vol. 55, pp. 1664–1674, Oct. 1967.
2) Gold, B. and Rader, C.M.: Digital Processing of Signals. New York: McGraw-Hill, 1969.
3) Hofstetter, E., Oppenheim, A.V. and Siegel, J.: "A new technique for the design of nonrecursive digital

filters," in Proc. 5th Annual Princeton Conf. Information Sciences and Systems, pp. 64–72, Mar. 1971.
4) Hirano, K., Nishimura, S. and Mitra, S.K.: "Design of digital notch filters," IEEE Trans. Circuit Syst., vol. CAS-21, pp. 540–546, July 1974.
5) Hirano, K., Saito, T., Nishimura, S. and Mitra, S.K.: "Time-sharing realization of digital Butterworth filters," Monograph of Circuit and Systems Society of IECE of Japan, Dec. 1973.
6) Hu, J.V. and Rabiner, L.R.: "Design techniques for two-dimensional digital filters," IEEE Trans. Audio Electroacoust., vol. AU-20, pp. 88–89, Mar. 1972.
7) Iinuma, T. and Nagai, T.: "Image restoration in radioisotope imaging systems," Phys. Med. Biol. 12: p. 501, 1967.
8) MacIntyre, W.J. and Christie, J.H.: "A comparison of data averaging of radioisotope scan data by photographic and dimensional computer techniques," Medical Radioisotope Scintigraphy (Salzburg: I.A.E.A.) 1: p. 771, 1969.
9) Kaiser, J.F.: "Digital filters," in System Analysis by Digital Computer, Kuo, F.F. and Kaiser, J.F., Eds. New York: Wiley, 1966, ch. 7.
10) Matsuo, M.: "An Application of linear phase IIR digital filtering to processing of the scintigraphic image." will be published.
11) Mitra, S.K. and Hirano, K.: "Multiplier extraction approach," presented at the Arden House Workshop, Jan. 1974.
12) Mitra, S.K. and Hirano, K.: "Digital all-pass networks," IEEE Trans. Circuit Syst., vol. CAS-21, pp. 688–700, Sept. 1974.
13) Mitra, S.K., Hirano, K. and Sakaguchi, H.: "A simple method of computing the input quantization and multiplication roundoff errors in a digital filter," IEEE Trans. Acoust., Speech, and Signal Processing, vol. ASSP-22, pp. 326–329, Oct. 1974.
14) Nagai, T., Fukuda, N. and Iinuma, T.: "Computer-focusing using an appropriate gaussian function," J. Nucl. Med. 10: p. 209, 1969.
15) Nagai, T. and Iinuma, T.: "A comparison of differential and integral scans," J. Nucl. Med. 9: p. 202, 1968.
16) Parks, T.W. and McClellan, J.H.: "Chebyshev approximation for nonrecursive digital filters with linear phase," IEEE Trans. Circuit Theory, vol. CT-19, pp. 189–194, Mar. 1972.
17) Rabiner, L.R.: "Techniques for designing finite-duration impulse-response digital filters," IEEE Trans. Commun. Technol., vol. COM-19, pp. 188–195, Apr. 1971.
18) Rabiner, L.R.: "The design of finite impulse response digital filters using linear programming techniques," Bell Syst. Tech. J., vol. 51, pp. 1177–1198, Aug. 1972.
19) Rabiner, L.R. and Gold, B.: Theory and Application of Digital Signal Processing, Englewood Cliffs, N.J.: Prentice-Hall, 1975.
20) Rabiner, L.R., Gold, B. and McGonegal, C.A.: "An approach to the approximation problem for nonrecursive digital filters," IEEE Trans. Audio Electroacoust., vol. AU-18, pp. 83–106, June 1970.
21) Rabiner, L.R., Graham, N.Y. and Helms, H.D.: "Linear programming design of IIR digital filters with arbitrary magnitude function," IEEE Trans. Acoust., Speech, and Signal Processing, vol. ASSP-22, pp. 117–123, Apr. 1974.
22) Rader, C.M. and Gold, B.: "Digital filter design techniques in the frequency domain," Proc. IEEE, vol. 55, pp. 149–171, Feb. 1967.
23) Schuessler, H.W.: "On the approximation problem in the design of digital filters," in Proc. 5th Annual Princeton Conf. Information Sciences and Systems, pp. 54–63, Mar. 1971.
24) Selzer, R.H.: "Improving biomedical image quality with computers," NASA Tech. Rep., pp. 1332–1336, 1968.
25) Shanks, J.L. and Justice, J.H.: "Stability and synthesis of two-dimensional recursive filters," IEEE Trans. Audio Electroacoust., vol. AU-20, pp. 249–257, Oct. 1972.
26) Tanaka, E. and Iinuma, T.: "Approaches to optimal data processing in radioisotope imaging," Phys. Med. Biol. 15: p. 683, 1970.
27) Treitel, S., Shanks, L. and Frasier, C.W.: "Some aspect of fan filtering," *Geophysics*, vol. 32, pp. 789–800, Oct. 1967.
28) Wilensky, S., Ashare, A.B., Pizer, S.M., Hoop, B. and Brownell, G.L.: "Computer processing and display of positron scintigrams and dynamic function curves," in Medical Radioisotope Scintigraphy (Salzburg: I.A.E.A.) 1: p. 815, 1969.
29) Zurflueh, E.G.: "Applications of two-dimensional linear wavelength filtering," Geophysics, vol. 32, pp. 1015–1035, Dec. 1967.